ECS Transactions, 52 (1) 941-946 (2013)
10.1149/05201.0941ecst ©The Electrochemical Society

Characterization of Random Telegraph Noise in Scaled High-κ/Metal-gate MOSFETs with SiO_2/HfO_2 Gate Dielectrics

Meng Li, Runsheng Wang*, Jibin Zou, Ru Huang*

Institute of Microelectronics, Peking University, Beijing 100871, China

*Email: ruhuang@pku.edu.cn, r.wang@pku.edu.cn

In the paper, random telegraph noise (RTN) in high-κ/metal-gate MOSFETs is investigated. The RTN in high-κ MOSFETs is found different compared to that in SiON MOSFETs, and faces challenges in characterization. Therefore, the characterization method is improved based on clustering and Hidden Markov Model, which greatly enhances the ability to extract RTN with non-negligible "ghost noise" in high-κ MOSFETs. The RTN signal and "ghost noise" in devices fabricated by two SiO_2/HfO_2 stack processes with two different formation methods are compared. It is found that the real RTN signal in SiO_2/HfO_2 MOSFETs originates from the oxide defects in the HfO_2 layer, while the "ghost noise" originates from the SiO_2 interfacial layer and has strong dependence on the quality and formation process of interfacial layer.

Introduction

Recently, the random telegraph noise (RTN) has attracted much attention in nanoscale devices and circuits[1-12], because RTN amplitudes increase rapidly as device scaling and directly degrades circuit variability and reliability. Therefore, the characterization of RTN is becoming important for new technology. In the paper, RTN in high-κ/metal-gate technology is characterized and analyzed. The RTN characteristics in scaled MOSFETs with SiO_2/HfO_2 gate dielectrics are found different compared to that in SiON devices, as shown in Fig. 1 and thus the traditional method is not applicable. Therefore, the characterization method of RTN is improved in this paper. Then the process dependence and the origin of RTN and "ghost noise" in SiO_2/HfO_2 devices are also investigated.

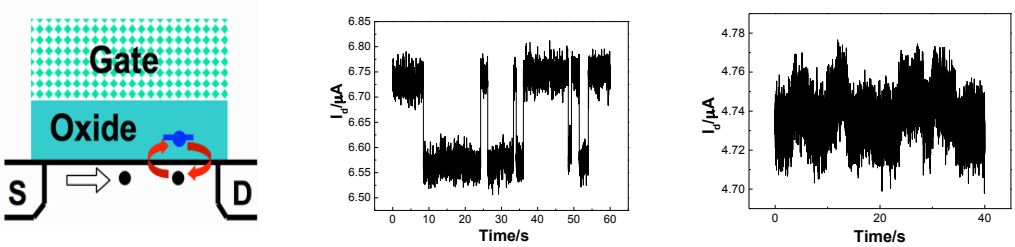

(a) (b) (c)

Figure 1. (a) Illustration of the RTN signal generation. (b) Typical RTN signal in SiON MOSFETs. (c) Typical RTN signal in high-κ/metal-gate MOSFETs.

RTN characterization for high-κ/metal-gate MOSFETs

The characterization of RTN in SiO_2/HfO_2 MOSFETs is challenging since in a large fraction (>50%) of the devices, there is a non-negligible "ghost noise" signal behind the actual RTN signal from our experiments; while the RTN signals in conventional SiO_2 or SiON devices are very clear, as shown in Fig. 1(b) and Fig. 1(c). Traditionally, to extract the RTN signal, people simply set a threshold artificially or fit the data to Gaussian distribution[13]. However, this method is limited by the amplitude of noise signal as shown in Fig.2(a).

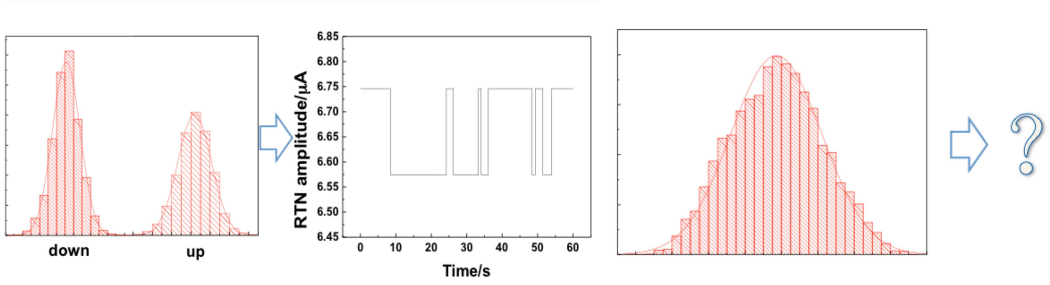

(a) (b)

Figure 2. Characterization of RTN signal using traditional method. (a) The histogram and RTN signal for Fig. 1(b). (b) The histogram for high-κ/metal-gate RTN signal in Fig. 1(c).

Therefore, when the amplitude of "ghost noise" is large enough, the RTN signal cannot be extracted correctly using the traditional method as shown in Fig. 2(b). From our data, we noticed that "ghost noise" obeys Gaussian statistics in most situations. Considering that, in theory, the RTN statistics is actually a typical Markov process (Poisson process)[1,9], thus by using the improved method based on Hidden Markov Mode (HMM)[7,14,15] , which has been widely used in speech recognition[17], we can successfully extract the RTN signal from the "noisy" data. The improved method is shown in Fig. 3.

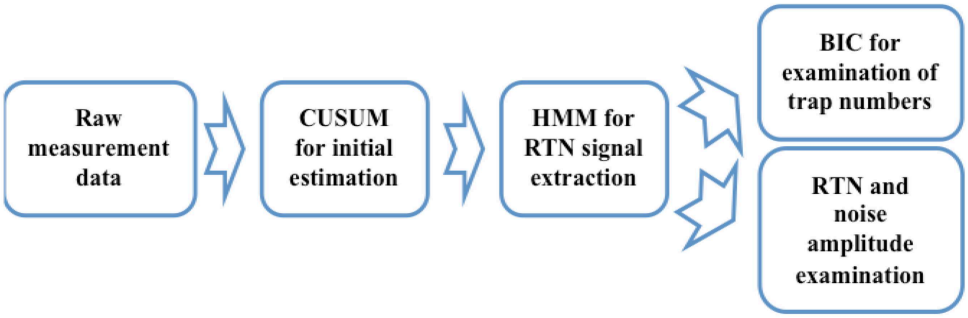

Figure 3. Flow chart of improved method for RTN signal characterization

Initial estimation For HMM, we make use of numerical calculation and thus, the computation increases rapidly with the amount of data becoming larger. Meanwhile, the initial estimation of parameters like RTN amplitude and noise standard deviation could influence the final result as well. Therefore, good priori estimation for current levels and "ghost noise" standard is important. Traditionally, histogram is used as initial estimation as shown in Fig. 2(a), which is greatly limited by the noise amplitude. In our method, we

make use of cumulative sum chart (CUSUM)[16] and by dividing and clustering to make the sum of intra-class distance the lest, we could get a preliminary RTN image and a reasonable initial estimation as shown in Fig. 4(b). Of course if the "ghost noise" is small enough, we could just use CUSUM itself to extracted RTN signal as well.

RTN extraction using HMM By using the characteristics of RTN and "ghost noise" as well as the initial estimation of crucial parameters, we could use HMM to get the RTN signal from the experimental data, as shown in Fig. 4(c). And we can get the "ghost noise" at the same time, as shown in Fig. 4(e).

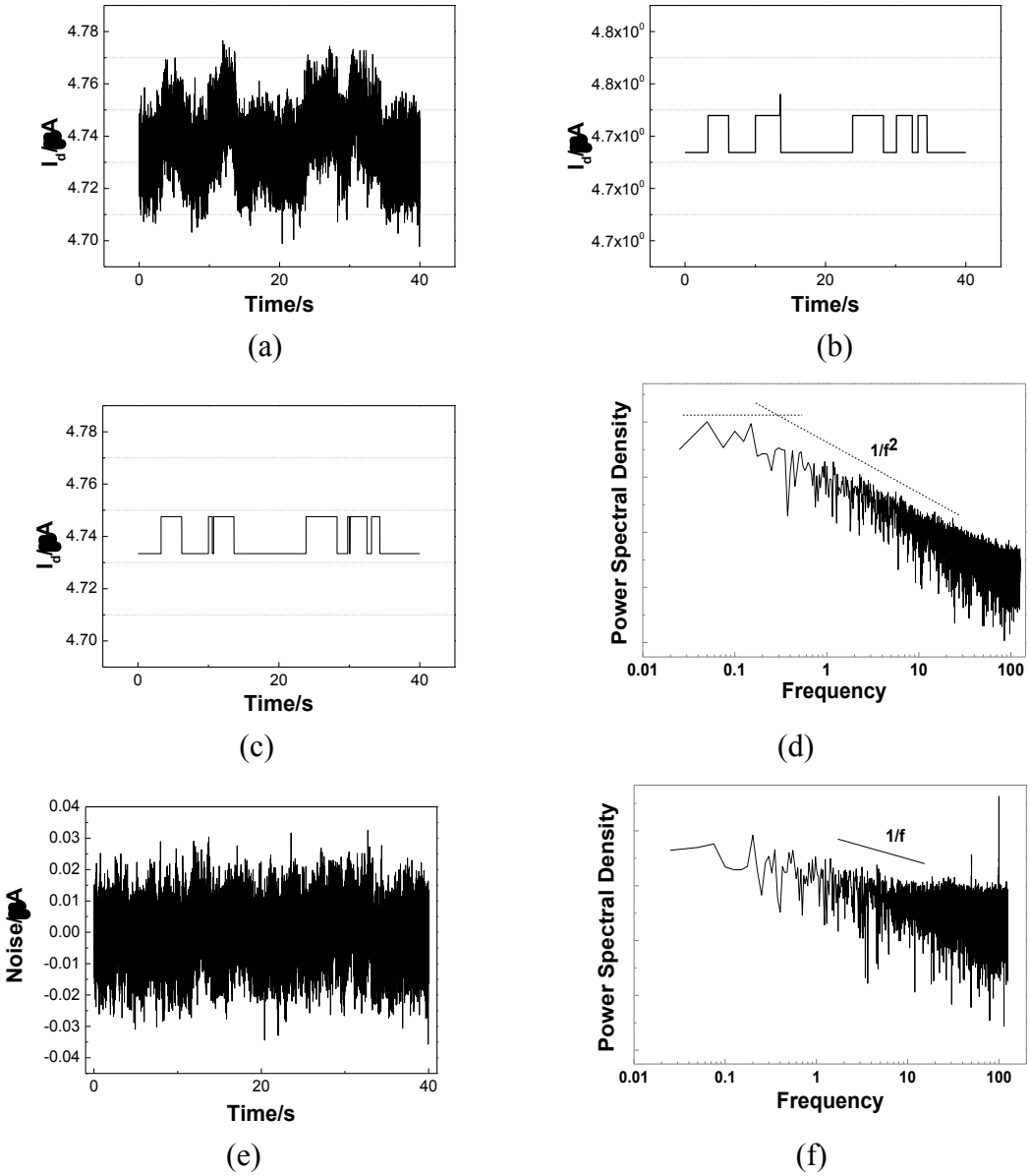

Figure 4. (a) Raw data of RTN measurement. (b) Preliminary RTN signal extracted using CUSUM, which could be initial estimation of HMM. (c) Final RTN signal extracted using Hidden Markov Model, which has improved accuracy than the initial estimation of (b). (d) The power spectral density of the extracted RTN. (e) "Ghost noise" extracted from raw data. (f) The power spectral density of the extracted "ghost noise"

Posteriori examination The HMM could be regarded as non-supervision machine learning. Therefore, both the accuracy of the final result and the number of traps should be examined after the extraction of RTN signal.

Traditionally, time lag plot (TLP) is used to get the number of traps as a priori knowledge[18,14], which may be limited by the amplitude of the noise. In our method, we use Bayesian Information Criterion (BIC)[19] to act as a posteriori check of our work.

The equation of BIC is

$$BIC = -2 \times \ln(L) + k \times \ln(n)$$

where L stands for the maximized value of the likelihood function for the estimated model, k stands for the number of free parameters to be estimated and n stands for the number of data points. The smaller the BIC index is, the better the description is. Therefore, using the equation above, we can get the most concise and relative accurate description of the measurement data.

As for accuracy examination, by extracting our artificially generated sequences and comparing the result with original Poisson sequences, we could set the supervision for the method and decide the applicable scope of it. From our test, if the amplitude of "ghost noise" (1σ) is smaller than 3 times of RTN signal (ΔI_d), we can correctly get the RTN from the measurement data. Therefore, this could act as a posteriori criterion for us to decide the accuracy of our characterization.

Results and Discussion

Using the improved method above, we can characterize the RTN signal and "ghost noise" for most of our measurement in high-κ/metal-gate devices.

We firstly examine the correlation of RTN signal and "ghost noise" from the following two aspects:

1) The correlation of "ghost noise" amplitude (1σ) and RTN signal amplitude ($\Delta I_d/I_d$).
2) The correlation of "ghost noise" amplitude (1σ) in defect occupancy state and defect empty state.

As indicated in Fig. 5 and Fig. 6, we can see that the amplitude of "ghost noise" has no correlation to the real RTN signal.

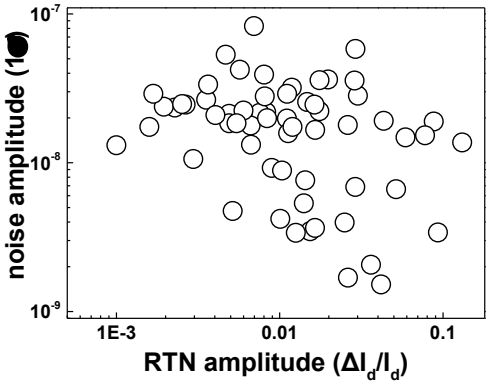

Figure 5. Non-correlation pattern between RTN and the "ghost noise"

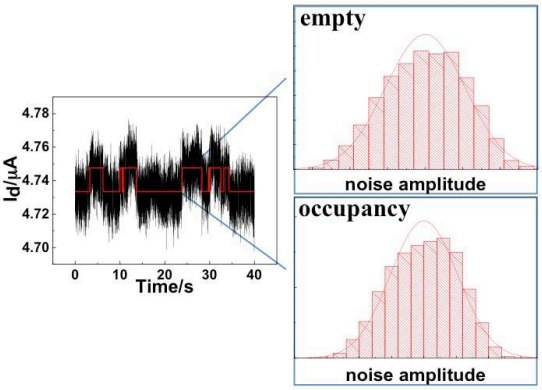

TABLE I. Comparison of "ghost noise" amplitude in different defect states

Noise Amplitude	Capture State	Emission State
Defect 1	1.3028×10^{-08}	1.3558×10^{-08}
Defect 2	1.3711×10^{-08}	1.3014×10^{-08}
Defect 3	1.0451×10^{-08}	1.0528×10^{-08}
Defect 4	1.2431×10^{-08}	1.2534×10^{-08}

Figure 6. Non-correlation pattern between noise amplitudes in two defect states

Since there is no direct correlation between RTN signal and "ghost noise", we can study the RTN signal and "ghost noise" separately. We compare the RTN signal and "ghost noise" for two SiO_2/HfO_2 stack processes (process A and process B) with two different formation methods for the SiO2 interfacial layer (IL). It is found that for process A, the amplitude of RTN is smaller and the amplitude of "ghost noise" is larger; while it is exactly the opposite for process B, as shown in Fig. 7.

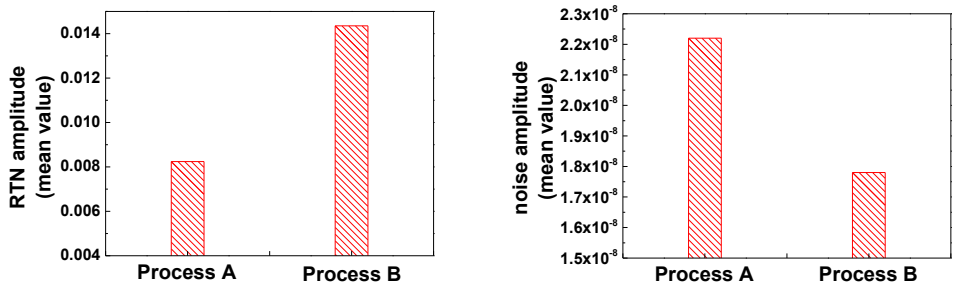

(a) (b)

Figure 7. Comparison of RTN amplitude and "ghost noise" amplitude between two high-κ stack processes (process A and process B).

From the comparison, we can conclude that the real RTN signal in SiO_2/HfO_2 MOSFETs originates from the oxide defects in the HfO_2 layer, and the "ghost noise" originates from the SiO_2 IL, which strongly depends on the IL quality and its formation process. Meanwhile, we can also get the conclusion that compared with process B, the IL quality of process A is worse but the high-κ oxide quality of process A is better.

Summary

Characterization of RTN signal in high-κ/metal gate MOSFETs is challenging due to non-negligible "ghost noise". In this paper, the improved method for RTN characterization is proposed and the origins of RTN signal and "ghost noise" in high-κ/metal gate MOSFETs as well as their correlation are studied. It is found that there is no direct correlation between RTN and "ghost noise". Furthermore, by comparing different IL fabrication methods of SiO_2/HfO_2 gate dielectric, it is concluded that RTN signal mainly originates from oxide defects in the HfO_2 layer, while the "ghost noise" originates from the SiO_2 IL and has a strong dependence on the IL quality and formation process.

Acknowledgement

The authors would like to thank Simeon Realov, H. Miki and Liangcai Gao for the helpful discussion on HMM. This work was supported in part by NSFC (61106085 and 60625403), the 973 Projects (2011CBA00601), National S&T Major Project (2009ZX02035-001) and Postdoctoral Science Foundation.

Reference

1. U. J. Uren, D. J. Kirton et al., *Appl Phys Lett,* **47**, 1195 (1985)
2. H . Kurata, K. Otsuga et al., *IEEE J. Solid-St Circ,* **42**, 1362 (2007)
3. J. Zhuge, L. Zhang et al. *Appl. Phys. Lett*, **94**, 083503 (2009)
4. L. Zhang, J. Zhuge et al., p.46, *VLSI Symp. Tech. Dig.*(2009)
5. K. Takeuchi et al., p.54, *VLSI Symp. Tech. Dig.*(2009)
6. C. Liu, R. Wang et al., p.521, *IEDM Tech. Dig.*(2009)
7. S. Realov and K. L. Shepard, p.624, *IEDM Tech. Dig.*, San Francisco, CA (2010)
8. S. O. Toh et al., p.204, *VLSI Symp. Tech. Dig.*(2011)
9. T. Grasser, *Microelectronics Reliability,* **52**, 39 (2011)
10. R. Wang, J. Zou, p.T23, *Int. Symp. on VLSI Tech., Sys. and Appl.*, Taiwan (2012)
11. J. Zou, R. Wang et al., p.139, *VLSI Symp. Tech. Dig.* (2012)
12. N. Tega et al., p.50, *VLSI Symp.,* Kyoto (2009)
13. Y. Yuzhelevski, M. Yuzhelevski et al., *R. of Sci. Instru.,* **71,** 1681(2000)
14. H. Miki et al., p.148, *VLSI Symp.* (2011)
15. D. J. Frank, *Int. Rel. Phys. Symp. Tutorial* (2012)
16. D. Brook and D.A. Evans, *Life Sci. & Math. & Phys. Sci.,* **59**, 539 (1972)
17. L. R. Rabiner, *Proceedings of the IEEE,* **77**, 257 (1989)
18. T. Nagumo, K. Takeuchi et al., p.759, *IEDM Tech. Dig.*, Baltimore (2009)
19. S. S. Chen, *Acoustics, Speech and Signal Prcessoing*, **2**, 645 (1998)